Using artificial intelligence to monitor live fuel moisture content across France, based on a high resolution land surface analysis - Supplements

Yann Baehr[1], Pierre Vanderbecken[1], Bertrand Bonan[1], Catherine Robert[2], Mathieu Regimbeau[3], François Pimont[4], Kevyn Raynal[4], Xiangzhuo Liu[5], Remi Savazzi[7], Moncef Garouani[8], Josiane Mothe[9], Nemesio Rodriguez-Fernandez[6], Lionel Jarlan[6], and Jean-Christophe Calvet[1]

[1]Météo-France, CNRS, Univ. Toulouse, CNRM, Toulouse, France
[2]Météo-France, Direction des Opérations pour la Prévision, Coordination nationale feux de végétation, Toulouse, France
[3]Météo-France, Direction des Services Météorologiques, Division Agrométéorologie, Toulouse, France
[4]INRAE, URFM, Avignon, France
[5]INRAE, UMR1391 ISPA, Villenave d'Ornon, France
[7]ONF, pôle national DFCI, Direction territoriale Midi-Méditerranée, Aix-en-Provence, France
[6]CESBIO, University of Toulouse, IRD/CNRS/UPS/CNES, Toulouse, France
[8]IRIT, Univ. Toulouse Capitole, UMR5505 CNRS, Toulouse, France
[9]IRIT, UT2J, Univ. de Toulouse, UMR5505 CNRS, Toulouse, France

Correspondence: Jean-Christophe Calvet (jean-christophe.calvet@meteo.fr)

This Supplementary Material provides additional figures, tables, and methodological details supporting the results presented in the main article.

Supplement 1: ONF field sites and species

Full description of the ONF (*Réseau Hydrique*) monitoring network, including site coordinates, vegetation types, and species sampled. Table S1 lists all sites and their corresponding dominant species.

Table S1. List of georeferenced sites of the *Réseau Hydrique* available in the database. The site code provides an identifier of the form "DmSn" where m is the "département" number (i.e. administrative county) and n, the site number within a "département".

Site Code	Site Name	X(°)	Y(°)	Sampled Species	Sample size	Period	RMSE (%)	KGE	NSE	R
D01S1	Parves et Nattages	5.75	48.70	*Coronilla emerus* *Rubus ulmifolius*	14	2024	21.12	-0.06	-3.18	0.73
D04S1	Les Adrechs	5.92	44.03	*Genista cinerea*, *Rosmarinus officinalis*	846	1996-2024	8.29	0.92	0.91	0.97
D04S2	Les Pailles	6.50	43.98	*Buxus sempervirens*, *Genista cinerea*	740	1996-2024	11.89	0.80	0.61	0.94

Continued on next page

Site Code	Site Name	X(°)	Y(°)	Sampled Species	Sample size	Period	RMSE (%)	KGE	NSE	R
D05S1	Théus	6.17	44.48	*Genista cinerea*, *Juniperus communis*	18	2024	11.33	0.88	0.77	0.99
D06S1	Lou Lambert	7.34	43.83	*Juniperus oxycedrus*, *Rosmarinus officinalis*	894	1996-2024	14.82	0.74	0.54	0.88
D06S2	Barbossi	6.90	43.53	*Acacia dealbata*, *Cistus monspeliensis*	889	1996-2024	17.75	0.39	-0.01	0.62
D06S3	Mouans-Sartoux	6.93	43.60	*Cistus salviifolius*, *Erica arborea*	22	2024	17.30	0.55	-0.37	0.76
D06S4	Carros	7.19	43.78	*Cistus albidus*, *Rosmarinus officinalis*	62	2022-2024	13.95	0.54	0.73	0.95
D07S1	Bois Sauvage	4.46	44.44	*Buxus sempervirens*, *Coronilla emerus* *Arbutus unedo*	229	2011-2024	10.12	0.76	0.75	0.87
D07S2	Annonay	4.63	45.22	*Calluna vulgaris*, *Genista purgans*, *Arbutus unedo*, *Erica scoparia*	426	1996-2024	34.46	0.42	-5.34	0.87
D09S1	Tarascon sur Ariège	1.59	42.86	*Genista scoparius*, *Rosa canina*	28	2023-2024	13.18	0.54	0.02	0.85
D11S1	Col de Nouvelle	2.79	42.91	*Quercus coccifera*, *Rosmarinus officinalis*	904	1996-2024	9.95	0.51	0.63	0.92
D11S2	Le Chemin des Bornes	2.92	43.12	*Cistus monspeliensis*, *Erica scoparia*	911	1996-2024	15.85	0.18	0.26	0.60
D11S3	La coumelle	2.68	43.08	*Quercus coccifera*, *Rosmarinus officinalis*	164	2018-2024	6.10	0.56	0.55	0.77
D11S4	Gruissan	3.06	43.12	*Quercus coccifera*, *Rosmarinus officinalis*	78	2022-2024	12.30	0.31	0.06	0.66
D11S5	Pouzols	2.79	43.28	*Cistus albidus*, *Quercus coccifera*	68	2022-2024	17.23	0.37	-0.52	0.74
D12S1	Millau	3.18	44.12	*Arctostaphylos uva-ursi*, *Juniperus communis*	17	2023-2024	9.98	0.88	0.58	0.93
D12S2	Fayet	2.96	43.80	*Cistus salviifolius*, *Erica arborea*	12	2024	13.35	0.62	0.34	0.66
D13S1	La Charlotte	5.06	43.69	*Quercus coccifera*, *Rosmarinus officinalis*, *Cistus albidus*, *Quercus ilex*	1047	1996-2024	16.48	0.45	0.36	0.68
D13S2	Le Romaron	5.16	43.35	*Quercus coccifera*, *Rosmarinus officinalis*	895	1997-2024	8.09	0.75	0.45	0.76
D13S3	Bouc-Bel-Air	5.44	43.46	*Cistus albidus*, *Rosmarinus officinalis*	62	2022-2024	20.58	0.22	-0.28	0.23

Continued on next page

Site Code	Site Name	X(°)	Y(°)	Sampled Species	Sample size	Period	RMSE (%)	KGE	NSE	R
D13S4	Cassis	5.57	43.21	*Cistus albidus*, *Rosmarinus officinalis*	64	2022-2024	12.92	0.61	0.72	0.92
D15S1	Ruynes en Margeride	3.22	44.99	*Cytisus scoparius*, *Juniperus communis*	12	2024	32.90	-0.07	-1.14	0.09
D16S1	Forêt de la braconne	0.29	45.78	*Erica scoparia*, *Spiraea hypericifolia*	34	2023-2024	14.52	0.83	0.62	0.91
D16S4	Rougnac	0.38	45.54	*Prunus spinosa*, *Spiraea hypericifolia* *Calluna vulgaris*, *Erica scoparia*	20	2024	56.27	0.36	-3.33	0.43
D17S1	Forêt de la coubre	-1.19	45.71	*Cistus salviifolius*, *Cytisus scoparius*	36	2023-2024	36.59	0.56	-0.78	0.89
D21S1	Châtillon	4.52	47.86	*Crataegus monogyna*, *Ligustrum vulgare*	13	2024	27.52	-0.22	-1.76	-0.03
D24S1	Montpon-Ménestérol	0.17	45.05	*Calluna vulgaris*, *Erica scoparia*	20	2024	30.74	0.59	-2.66	0.93
D24S2	Chalagnac	0.67	45.10	*Juniperus communis*, *Ligustrum vulgare*	16	2024	21.62	-3.24	-19.75	0.80
D26S2	Véronne	5.19	44.71	*Amelanchier lamarckii*, *Genista scoparius*	18	2024	30.93	-0.57	-14.36	0.79
D29S2	Monts d'Arrée	-4.00	48.36	*Cytisus scoparius*, *Erica cinerea*	14	2024	48.64	-0.69	-4.53	-0.49
D2AS1	Salario	8.70	41.92	*Cistus monspeliensis*, *Erica arborea*	963	1996-2024	13.89	0.62	0.59	0.77
D2AS2	FT Valle Mala	9.00	41.73	*Arbutus unedo*, *Erica arborea*	754	2000-2024	8.72	0.78	0.59	0.80
D2AS3	Lecci	9.32	41.65	*Cistus monspeliensis*, *Erica arborea*	339	2012-2024	20.18	0.50	0.21	0.67
D2AS4	Figari	9.10	41.47	*Arbutus unedo*, *Cistus monspeliensis*	52	2023-2024	15.33	0.25	0.00	0.38
D2BS1	Lancone C	9.41	42.64	*Cistus monspeliensis*, *Erica arborea*	22	2024	20.91	0.55	0.26	0.87
D2BS2	Quilico	9.17	42.33	*Cistus monspeliensis*, *Erica arborea*	766	2000-2024	15.30	0.13	-1.80	0.25
D2BS3	Bonifatu	8.84	42.44	*Cistus monspeliensis*, *Erica arborea*	777	1997-2024	20.53	0.57	-0.70	0.75
D2BS4	Aéroport de Calvi	8.80	42.52	*Cistus monspeliensis*, *Erica arborea*	60	2022-2024	14.26	0.33	0.24	0.57
D2BS5	Bocca di Vezzu	9.14	42.66	*Cistus monspeliensis*, *Erica arborea*	80	2022-2024	17.47	0.43	0.41	0.64
D2BS6	Serra-di-Fiumorbo	9.36	41.99	*Arbutus unedo*,	68	2022-2024	16.53	0.60	0.10	0.81

Continued on next page

Site Code	Site Name	X(°)	Y(°)	Sampled Species	Sample size	Period	RMSE (%)	KGE	NSE	R
D30S1	Roc du Bajanet	4.01	44.22	*Cistus monspeliensis*, *Erica cinerea*, *Erica scoparia*	716	1996-2024	13.47	0.49	0.41	0.89
D30S2	Le Télégraphe	4.42	43.88	*Cistus albidus*, *Quercus ilex*	1025	1996-2024	10.44	0.39	-0.98	0.47
D30S3	Conqueyrac	3.89	43.92	*Brachiaria ramosa*, *Buxus sempervirens* *Quercus coccifera* *Juniperus oxycedrus*, *Rosmarinus officinalis*	60	2022-2024	14.04	0.33	-0.41	0.82
D31S1	FD Bouconne	1.26	43.64	*Cistus salviifolius*, *Erica scoparia*	7	2024	58.53	-0.29	-0.57	-0.00
D33S1	Carcan	-1.14	45.09	*Cistus salviifolius*, *Erica scoparia*	34	2023-2024	20.76	0.62	0.31	0.78
D33S2A	Martignas-sur-Jalle	-0.79	44.85	*Calluna vulgaris*, *Cistus salviifolius*	23	2024	42.43	0.19	-3.56	0.78
D33S4	Le Porge	-1.19	44.86	*Cytisus scoparius*, *Erica scoparia*	38	2023-2024	23.24	0.70	0.40	0.80
D33S5A	Belin-Béliet	-0.82	44.52	*Calluna vulgaris*, *Erica cinerea*	20	2024	11.43	0.86	0.64	0.92
D34S1	Le Bousquet d'Orb	3.16	43.68	*Erica scoparia*, *Juniperus oxycedrus*	22	2024	11.54	0.69	0.50	0.94
D34S2	Le Puits de l'Aven	3.71	43.57	*Cistus albidus*, *Quercus coccifera*	791	1999-2024	8.67	0.47	-0.05	0.50
D34S3	Montblanc	3.34	43.37	*Cistus monspeliensis*, *Juniperus oxycedrus*	66	2022-2024	10.58	0.50	0.51	0.90
D35S2	Liffré	-1.57	48.18	*Calluna vulgaris*, *Rhamnus frangula*	16	2024	33.63	0.77	-3.76	0.94
D36S3	Arthon	1.68	46.72	*Calluna vulgaris*, *Erica cinerea*	22	2024	15.57	0.40	-0.28	0.65
D38S1	Saint Imier	5.83	45.26	*Cornus glabrata*, *Juniperus communis*	12	2024	17.55	0.06	-2.57	0.27
D40S1	Biscarrosse	-1.22	44.46	*Cistus salviifolius*, *Cytisus scoparius*	40	2023-2024	16.43	0.84	0.58	0.84
D40S2	Sabres	-0.76	44.12	*Calluna vulgaris*, *Erica cinerea*, *Ulex minor*	29	2023-2024	16.39	0.69	0.36	0.70
D40S3	Losse	-0.02	44.05	*Erica scoparia*, *Rhamnus frangula*	21	2023-2024	55.19	0.56	-3.49	0.88
D40S5	Saint-Vincent-de-Paul	-1.01	43.77	*Erica scoparia*, *Ulex europaeus*	27	2023-2024	34.57	0.52	-1.16	0.55

Continued on next page

Site Code	Site Name	X(°)	Y(°)	Sampled Species	Sample size	Period	RMSE (%)	KGE	NSE	R
D41S2	Neuvy	1.58	47.58	*Calluna vulgaris*, *Cytisus scoparius*	18	2024	34.06	0.34	-1.57	0.69
D43S1	RetThenac	4.02	45.20	*Calluna vulgaris*, *Genista purgans*	16	2024	64.58	0.17	-18.80	0.86
D46S1	FD monclar	1.67	44.49	*Jasminum fruticans*, *Phillyrea latifolia*	15	2024	39.57	0.10	-0.09	0.42
D47S3A	Pompiey	0.18	44.20	*Cytisus scoparius*, *Erica scoparia*	19	2024	50.30	0.50	-0.53	0.94
D48S1	Boussal	3.94	44.43	*Calluna vulgaris*, *Genista purgans*	612	1997-2024	17.39	-2.15	-15.38	0.12
D48S2	Vallée Francaise	3.82	44.15	*Calluna vulgaris*, *Juniperus oxycedrus*	52	2022-2024	7.05	0.44	0.48	0.96
D56S3	Plouhinec	-3.22	47.68	*Erica cinerea*, *Ulex europaeus*	15	2024	48.08	0.43	-1.34	0.54
D61S2	Saint-Nicolas-Des-Bois	0.05	43.51	*Calluna vulgaris*, *Vaccinium myrtillus*	14	2024	27.79	0.20	-0.19	0.67
D64S1	Anglet	-1.50	43.51	*Cistus salviifolius*, *Cytisus scoparius*, *Ulex europaeus*	33	2023-2024	14.48	0.88	0.81	0.95
D66S1	Le Mas Péricot	2.87	42.51	*Cistus monspeliensis*, *Erica arborea*	822	1999-2024	16.70	0.21	0.05	0.84
D66S2	Le Vigné	2.47	42.64	*Cistus monspeliensis*, *Juniperus oxycedrus* *Cytisus scoparius*	884	1996-2024	20.70	0.48	-0.36	0.61
D66S3	Pezilla	2.75	42.71	*Cistus monspeliensis*, *Erica arborea*	28	2024	13.50	0.34	0.19	0.78
D66S4	Estavar	2.00	42.48	*Genista purgans*, *Juniperus communis*	22	2023-2024	27.84	0.41	-1.11	0.74
D68S1	Wittelsheim	7.21	47.79	*Crataegus monogyna*, *Cytisus scoparius*	13	2024	44.88	-0.30	-2.24	-0.26
D72S2	Marigne-Laille	0.35	47.78	*Calluna vulgaris*, *Cytisus scoparius*	18	2024	30.25	0.07	-0.06	0.23
D73S1	Notre Dame du Cruet	6.28	45.37	*Hippophae rhamnoides*, *Rosa canina*	14	2024	15.87	0.43	0.20	0.52
D76S2	Oissel	1.07	49.35	*Calluna vulgaris*, *Cytisus scoparius*	2	2024	Ø	Ø	Ø	Ø
D77S1	Fontainebleau	2.62	48.39	*Calluna vulgaris*, *Erica cinerea*	22	2024	34.19	-0.17	-3.06	-0.06
D79S3	Chizé	-0.36	46.12	*Crataegus monogyna*, *Ligustrum vulgare*	22	2024	27.19	0.67	-0.55	0.72
D82S1	St-antonin-noble-val	1.76	44.14	*Buxus sempervirens*,	10	2024	112.90	-0.46	-1.78	-0.21

Continued on next page

Site Code	Site Name	X(°)	Y(°)	Sampled Species	Sample size	Period	RMSE (%)	KGE	NSE	R
D83S1	Le Castellet	5.80	43.24	*Juniperus communis* *Cistus monspeliensis*, *Erica arborea*	903	1996-2024	19.82	0.40	0.10	0.58
D83S2	Le Haras du Rastéou	6.48	43.47	*Cistus albidus*, *Quercus ilex*	915	1996-2024	11.41	0.75	-0.33	0.78
D83S3	La Carrière du Juge	5.99	43.42	*Cistus albidus*, *Cistus monspeliensis*	863	1997-2024	18.95	0.39	0.45	0.79
D83S4	Pont Des Caunes	6.36	43.18	*Cistus monspeliensis*, *Erica arborea*	168	2018-2024	10.53	0.57	0.62	0.83
D83S5	Gonfaron	6.32	43.31	*Erica arborea*, *Juniperus communis*	71	2022-2024	7.10	0.48	0.36	0.61
D84S1	Mur de la Peste	5.14	43.90	*Cistus albidus*, *Quercus coccifera* *Quercus ilex*	862	1996-2024	Ø	Ø	Ø	Ø
D84S2	Peyrasse	5.61	43.73	*Quercus ilex*, *Rosmarinus officinalis*	920	1996-2024	25.11	-0.83	-4.19	0.71
D84S3	Cheval-Blanc	5.17	43.76	*Cistus albidus*, *Rosmarinus officinalis*	20	2024	24.38	0.13	0.10	0.44
D86S1	Verneil-Sur-Indre	0.52	46.69	*Calluna vulgaris*, *Erica scoparia*	63	2023-2024	37.35	0.29	-0.99	0.50

Supplement 2: Statics and dynamics ISBA predictors

Figure S1 shows maps of metadata extracted from ISBA-LDAS-AROME, including field capacity (WFC in m^3/m^3), sand fraction (%), orography (m) and rugosity (topographic standard deviation in m). These are followed by the dynamic inputs, which are also used as predictors in the neural network. Figure S2 (a) shows the SWI at the third soil layer (10 m in depth), Fig. S2 (b) illustrates the leaf area index (LAI in m^2/m^2), and Fig. S2 (c) presents the normalised LAI with the WFC. This figure shows how the dynamic inputs change as a function of the weather conditions by comparing the same variable for two given dates.

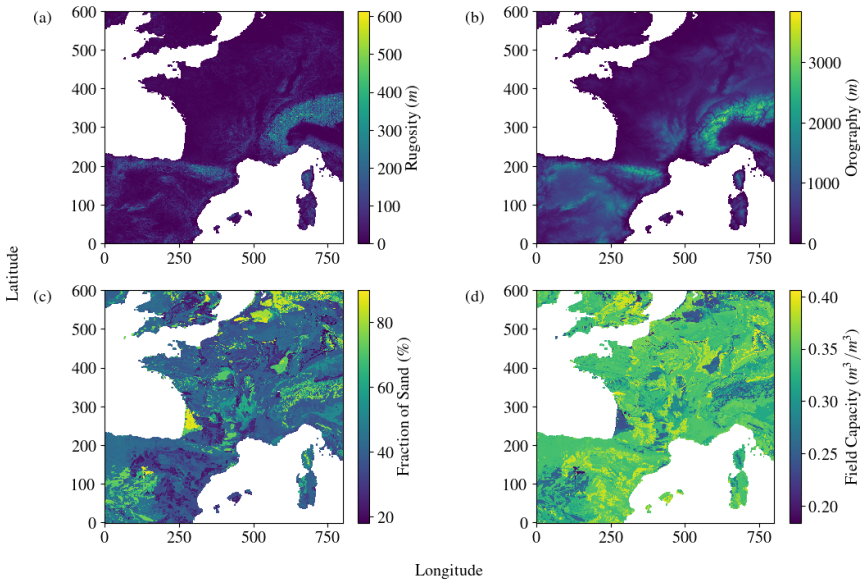

Figure S1. Spatial distribution of metadata extracted from ISBA used as model predictors. Four of them are presented: Rugosity in m (a), Orography in m (b), Fraction of sand in % (c) and Field capacity in m^3/m^3 (d).

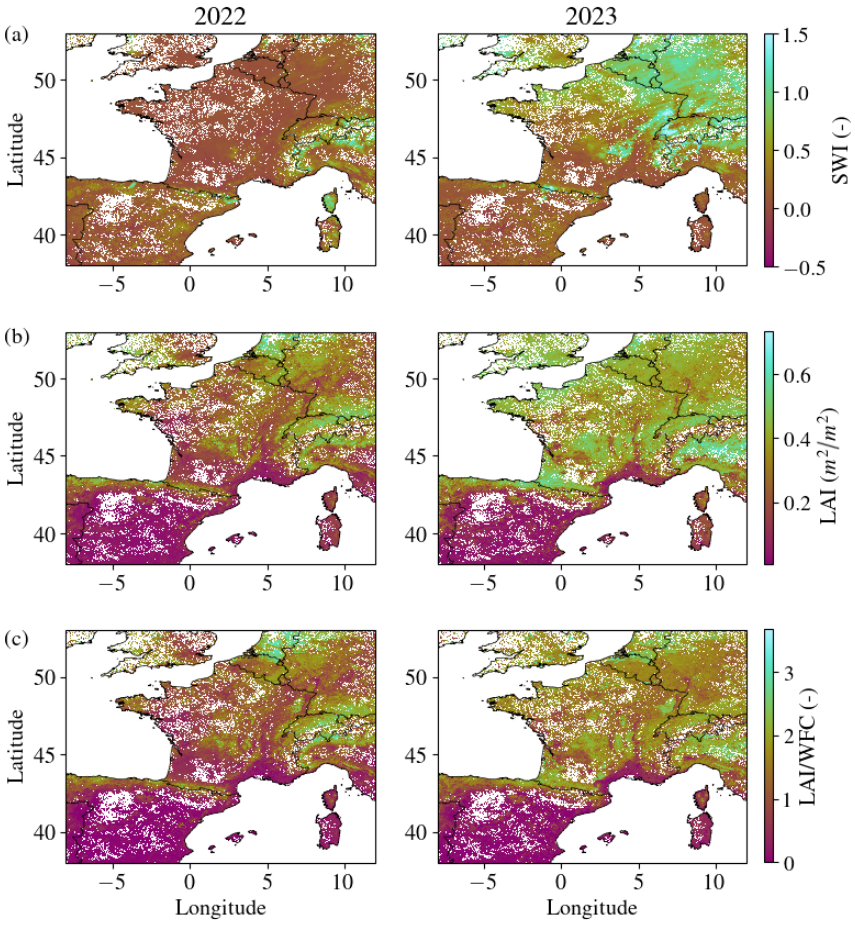

Figure S2. Spatial distribution of dynamic inputs from ISBA used as model predictors, comparing August 13 of 2022 and 2023. For the SWI (a), the LAI in m^2/m^2 (b) and the LAI normalised by the WFC (c).

Supplement 3: Model evaluation on 2024: temporal and spatial extrapolation

Table S2 is a summary of both performances of the model over the extended *Réseau hydrique* observations and the historical sites of the network (sites present in the training set). As we can see, the model has strong performance to represent the average of all the historical sites and manages to have a better degree of defining the fluctuation of the values through time.

Despite everything, the model struggles to capture temporal anomalies to the same extent as for the extended network. This lacks extremum search, which could be mitigated by making greater use of temporal depth, for example, contextual temporal variables using an LSTM, a temporal convolutional network, or post-processing of site-specific anomalies with site-by-site temporal calibration.

Also, there are two definitions of LFMC. Figure S3 presents the scores of the $\text{LFMC}_{\text{fresh}}$, which is the one used to calibrate the model. And Table S2 summarises scores between $\text{LFMC}_{\text{fresh}}$ and LFMC. Switching from $\text{LFMC}_{\text{fresh}}$ to LFMC_{dry} tends to amplify the extremes, which is why there has been a drop in performance.

Table S2. Model performance across spatial and temporal aspects computed on the full 2024 test set. First, over the entire set, secondly over the historical area of the Réseau Hydrique, thirdly based on the LFMC_{fresh} used by the ONF and operational services.

LFMC evaluation experiment	RMSE $\%$	KGE	NSE	Pearson R	Number of points
Neural network prediction over 2024					
`Overall performances`	25.2	0.70	0.62	0.79	916
`Site-averaged`	17.5	0.76	0.74	0.87	92
`Temporal anomalies`	4.0	0.37	0.38	0.63	916
Neural network prediction over sites present in the training set					
`Overall performances`	16.9	0.77	0.70	0.84	916
`Site-averaged`	9.2	0.86	0.85	0.93	92
`Temporal anomalies`	4.1	0.36	0.44	0.67	916
Neural network prediction over 2024 exprimed in $\text{LFMC}_{\text{fresh}}$					
`Overall performances`	5.4	0.74	0.66	0.81	916
`Site-averaged`	3.8	0.81	0.77	0.88	92
`Temporal anomalies`	3.9	0.55	0.38	0.63	916

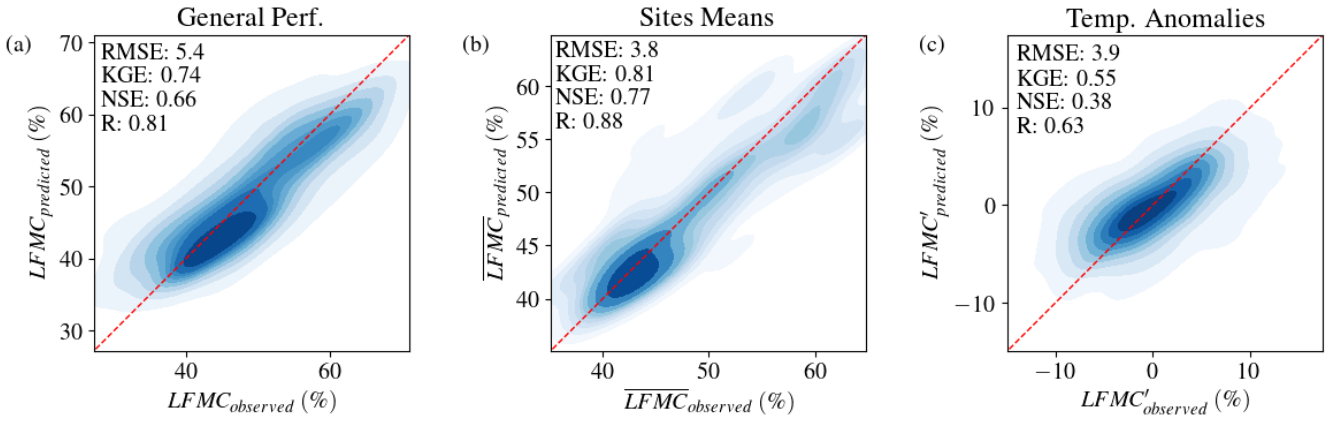

Figure S3. Scatter plots (joint density) of $LFMC_{fresh}$ predictions vs. observations for the 2024 test set. (a) General Performances, (b) Sites Means, (c) Temporal correlation

25

Supplement 4: Selection of the reference drought day

The date of 13 August 2022 was not chosen at random. The neural network model was applied to the entire summer of 2022, and grid cells with unrealistic values were masked. The date with the lowest spatially averaged LFMC value across the AROME grid was then selected as the reference day. This corresponds to the minimum live fuel moisture content, as illustrated in Fig. S4.

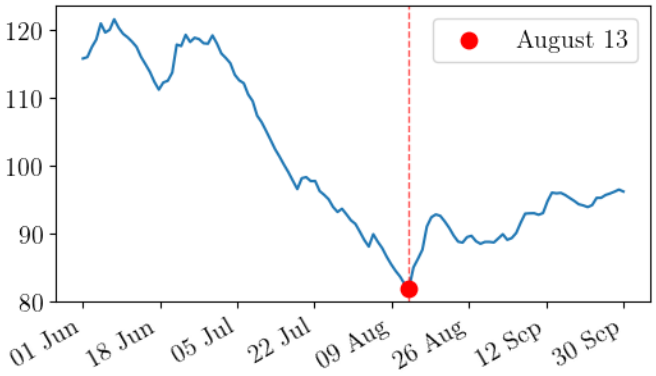

Figure S4. Spatially averaged LFMC evolution during summer 2022. The dashed vertical line indicates the date (13 August) corresponding to the minimum mean LFMC value over the domain.

Supplement 5: Effect of the number of parameters in the neural network

We investigate how model depth and latent dimensionality affect performance under different cross-validation schemes. Several neural network configurations were evaluated to assess the trade-off between model complexity and generalisation capability:

- Reference model — latent dimension of 4, approximately 7,000 parameters.
- Shallow 3-layer network — three dense layers (two of 32 units, one output), for a total of approximately 1,400 parameters, similar to the architecture used in Corchia (2024).
- Small latent model — The architecture with a latent dimension of 2, corresponding to 2,000 trainable parameters.
- Deep model — same structure with a latent dimension of 8, totalling 26,000 trainable parameters.

The results of all experiments, for the different validation strategies, are summarised in Table S3. The comparison highlights the influence of both model depth and the number of trainable parameters on predictive performance. Increasing model capacity improves the representation of complex spatio-temporal dependencies, but may also lead to overfitting when the number of parameters greatly exceeds the effective sample size. The intermediate configuration ($\sim 7,000$ parameters) was selected as the best compromise between expressivity and stability, ensuring a balanced ratio between model complexity and input feature dimensionality.

Table S3. Performance comparison between a three-layer neural network and the proposed neural network with varying latent dimensionalities (2, 4, and 8). The best score values are highlighted in bold.

Metric\Model	**The studied neural network**	**3-Layers neural network**	**The studied neural network** (small latent)	**The studied neural network** (big latent)
		Globals Performances		
RMSE (%)	**25.2**	28.3	26.4	26.5
KGE	0.70	0.66	**0.72**	0.64
NSE	**0.62**	0.52	0.58	0.58
Pearson R	**0.79**	0.73	0.78	**0.79**
		Forward Chaining		
RMSE (%)	**22.7**	27.5	22.9	**22.7**
KGE	**0.52**	0.03	0.50	0.51
NSE	0.08	-0.14	**0.12**	0.08
Pearson R	**0.59**	0.32	0.58	**0.59**
		Leave One Year Out		
RMSE (%)	18.5	23.3	18.7	**18.4**
KGE	**0.57**	0.29	0.53	**0.57**
NSE	**0.41**	0.15	0.40	**0.41**
Pearson R	**0.67**	0.51	**0.67**	**0.67**
		Leave One Site Out		
RMSE (%)	**20.3**	28.5	**20.3**	**20.3**
KGE	**0.58**	0.18	0.57	0.57
NSE	**0.40**	-2.19	0.39	**0.40**
Pearson R	0.72	0.59	**0.73**	0.72
		New 2024 ONF Sites		
RMSE (%)	**35.4**	40.6	36.7	36.2
KGE	0.47	0.42	0.43	**0.54**
NSE	**0.32**	0.11	0.27	0.29
Pearson R	**0.60**	0.49	0.57	0.58

Supplement 6: Canton scale of the French territory

Figure S5 presents the spatial delineation of the 2,378 French cantons as defined in the 2015 administrative zoning. The map is used as a reference spatial framework for the analyses presented in the study, providing a homogeneous partition of the territory. Available from IGN at https://geoservices.ign.fr/geofla.

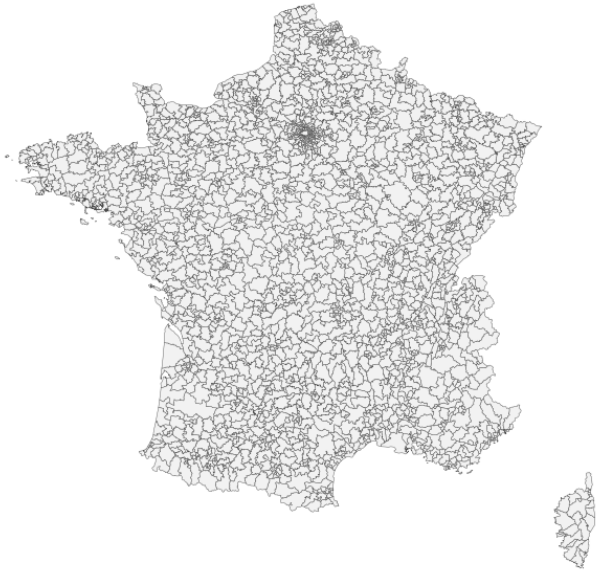

Figure S5. Spatial delineation of the French cantons (2015).

Supplement 7: Optimisation of station deployment strategy

We have introduced the rationale for expanding the ONF *Réseau Hydrique* network by using a prioritisation score that combines model uncertainty, the temporal variability of LFMC and the distance to existing sites. Here, we present the methodological details that underlie this prioritisation analysis.

For each AROME grid cell, an *Interest Score* (IS) was computed as a weighted combination of three spatial indicators:

$$IS = \alpha U + \beta \sigma_{LFMC} + \gamma D$$

where, U is the model uncertainty, quantified as the inter-model standard deviation of LFMC predictions obtained from multiple independent neural network trainings, σ_{LFMC} is the temporal standard deviation of LFMC, representing vegetation sensitivity to drought, D is the Euclidean distance to the nearest ONF field site, and α, β, and γ are weighting coefficients empirically set to balance the contribution of each component.

All predictors were first normalised to the [0, 1] range to avoid scale effects. Higher IS values thus correspond to regions where the model exhibits higher uncertainty, stronger seasonal variability, and lower observational constraints.

The computed IS field was subsequently classified using a K-means clustering (K = 2), resulting in three categories of interest:

1. **Low priority:** regions already well constrained by existing stations,
2. **High priority:** areas simultaneously exhibiting high model uncertainty and weak observational coverage.

This classification provides an objective spatial framework to guide the deployment of new monitoring stations, ensuring both spatial and ecological representativeness of the observational network.

The northern and north-western parts of France emerged as under-represented areas where additional LFMC observations would most improve model robustness. Conversely, southern France and Corsica already show dense observational coverage and consequently lower interest scores. This simple scoring approach demonstrates the potential of AI-based LFMC mapping to support data-driven network design and adaptive monitoring strategies.

Although the current approach is exploratory, it provides a solid foundation for future integration with formal *Optimal Sensor Placement* (OSP) techniques (Caselton and Zidek, 1984). OSP frameworks aim to identify observation locations that maximise information gain or minimise model uncertainty under spatial and logistic constraints. Incorporating such methodologies (e.g. entropy-based, variance reduction, or information-theoretic approaches) could transform the present heuristic IS formulation into a fully optimised decision-support system.

Future developments may also include additional variables such as vegetation type, accessibility, or fire risk indicators, allowing a multi-objective optimisation of the ONF monitoring network at the national scale.

Supplement 8: Impact of the day of the year

The Day of the Year (DOY) is one of the pieces of metadata used by the model to estimate LFMC. This information introduces seasonality, but this can be discussed.

We will therefore try to exclude this information from the training process in order to determine its influence on the scores. To do so, we will conduct another training 'without DOY'. First, however, we will compare the actual model with the full 2024 set, and then with the historical set (sites extracted from the training set).

As shown in Table S4, DOY contains a lot of information, and most scores decrease when temporal anomalies are considered, especially the KGE, which is highly sensitive to temporal dynamics. This suggests that the seasonality conveyed by this predictor cannot be ignored, particularly when no other temporal information is available. Figures S6 and S7 show how the model performs without DOY as a predictor for $LFMC_{fresh}$ and LFMC.

Table S4. Model performance across spatial and temporal aspects computed on the full 2024 test set. First, over the entire set and secondly over the historical area of the Réseau Hydrique, with and without the day of the year used as a predictor.

LFMC evaluation experiment	RMSE %	KGE	NSE	Pearson R	Number of points
All the set					
`Overall performances`	25.2	0.70	0.62	0.79	916
`Site-averaged`	17.5	0.76	0.74	0.87	92
`Temporal anomalies`	4.0	0.37	0.38	0.63	916
All the set without DOY					
`Overall performances`	26.8	0.68	0.57	0.76	916
`Site-averaged`	18.9	0.78	0.70	0.84	92
`Temporal anomalies`	4.1	0.22	0.33	0.58	916
Historical sites					
`Overall performances`	16.9	0.77	0.70	0.84	588
`Site-averaged`	9.2	0.86	0.85	0.93	52
`Temporal anomalies`	4.1	0.36	0.44	0.67	588
Historical sites without DOY					
`Overall performances`	17.3	0.72	0.69	0.83	588
`Site-averaged`	9.3	0.84	0.85	0.92	52
`Temporal anomalies`	4.1	0.23	0.42	0.65	588

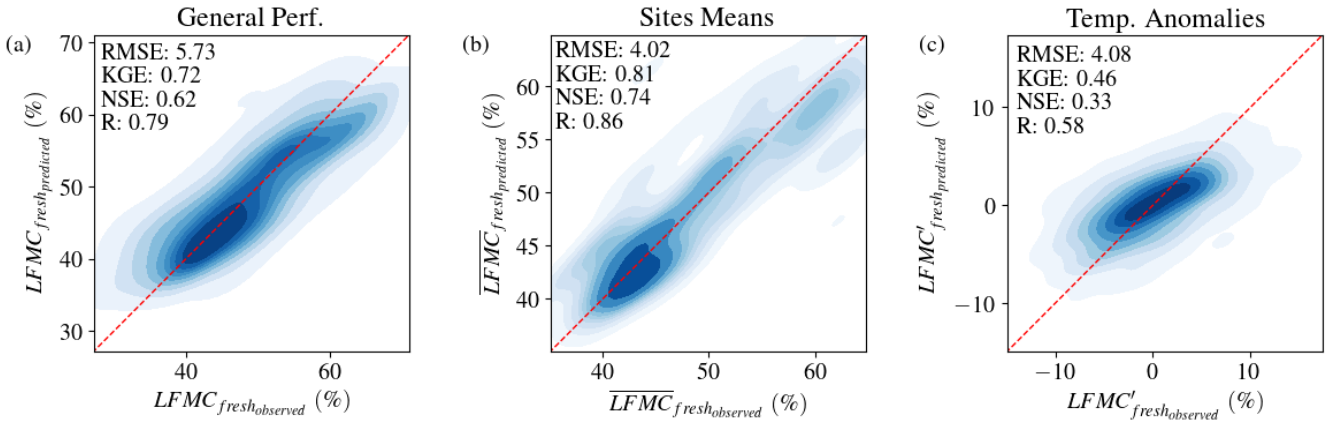

Figure S6. Scatter plots of $LFMC_{fresh}$ without the DOY predictions vs. observations for the 2024 test set. (a) General Performances, (b) Sites Means, (c) Temporal correlation

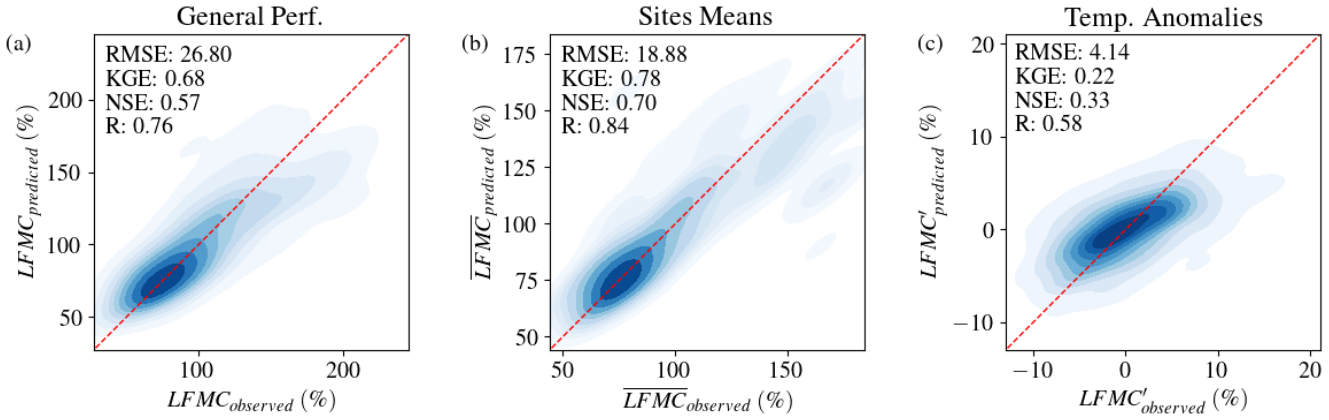

Figure S7. Scatter plots of LFMC without the DOY predictions vs. observations for the 2024 test set. (a) General Performances, (b) Sites Means, (c) Temporal correlation

References

Caselton, W. and Zidek, J.: Optimal monitoring network designs, Statistics Probability Letters, 2, https://doi.org/10.1016/0167-7152(84)90020-8, 1984.

Corchia, T.: Contribution of machine learning to the integration of satellite observations into a global model of the soil-plant system, Theses, Université de Toulouse, https://theses.hal.science/tel-04848876, 2024.